Supplemental Information for

A *Trans*-Hyponitrite Intermediate in the Reductive Coupling and Deoxygenation of Nitric Oxide by a Tricopper-Lewis Acid Complex

Davide Lionetti, Graham de Ruiter, and Theodor Agapie*

Division of Chemistry and Chemical Engineering, California Institute of Technology, 1200 East California Boulevard, MC 127-72, Pasadena, California 91125, United States

Contents

Experimental Section

General Considerations

Unless indicated otherwise, reactions performed under inert atmosphere were carried out in oven-dried glassware in a glovebox under a nitrogen atmosphere. Anhydrous tetrahydrofuran (THF) was purchased from Aldrich in 18 L Pure-Pac^{TM} containers. Anhydrous diethyl ether, acetonitrile, and THF were purified by sparging with nitrogen for 15 minutes and then passing under nitrogen pressure through a column of activated A2 alumina (Zapp's). Propionitrile was dried over

calcium hydride and vacuum transferred over molecular sieves. CD_3CN was purchased from Cambridge Isotope Laboratories, dried over calcium hydride, degassed by three freeze-pump-thaw cycles, and vacuum-transferred prior to use. ^1H NMR spectra were recorded on a Varian 300 MHz instrument, with shifts reported relative to the residual solvent peak. ^{19}F NMR spectra were recorded on a Varian 300 MHz instrument, with shifts reported relative to the internal lock signal. Electrospray ionization mass spectrometry (ESI-MS) was performed in the positive ion mode using a LCQ ion trap mass spectrometer (Thermo) at the California Institute of Technology Mass Spectrometry Facility. The ATR-IR measurements were recorded on a Bruker APLHA ATR-IR spectrometer at 2 cm^{-1} resolution using the OPUS software package. The gas-phase IR measurements were recorded on a Bio-Rad Excalibur Series spectrometer using a custom-made Schlenk cell fitted with KBr windows (pathlength = 10 cm). GC-MS analysis was performed on an Agilent 6890 gas chromatogram equipped with an Agilent 5793 mass-selective detector and an Agilent 19091S-433 column, using a 1.0 mL/min flow (He) and a 50 °C oven temperature. UV-Vis spectra were collected on a Varian 50Bio spectrophotometer using a Schlenk-adapted 1 cm quartz cuvette. Low-temperature UV-Vis spectra were obtained using a Varian dip-probe (661.202-UV, 10 mm) and a custom-made glass vessel Elemental analyses were performed by Midwest Microlab, LLC. (Indianapolis, IN). The EPR spectrum of **2** was obtained on an X-band EPR spectrometer and simulated using the EasySpin package for Matlab.[1] Unless indicated otherwise, all commercial chemicals were used as received. Nitric oxide was purchased from Aldrich. ^{15}NO was purchased from Cambridge Isotope Laboratories Complexes **1** and **3** were prepared according to previously published procedures.[2] Identical ^1H-NMR spectra were obtained with purified nitric oxide (NO), which was purified by careful distillation from pentane/liquid nitrogen at -115 °C (Figure S12); according to a modification of a procedure reported by Karlin and co-workers.[3] In short, on a high-vacuum manifold, nitric oxide was frozen in a 1L schlenk-tube at -196 °C, and heated to -115 °C in a pentane/liquid nitrogen bath. Once distillation commences, it is important to keep the distillation time short (< 30 sec.) in order to prevent N_2O contamination. The evolved gas was collected in a trap cooled at -196 °C. This procedure was repeated three times, and the purified nitric oxide was stored in a 500 mL glass bulb, fitted with Teflon valve, at reduced pressure.

Synthesis of 2.

In a Schlenk tube, a solution of **1** (0.212 g, 0.107 mmol) in EtCN (8 mL) was degassed by three freeze-pump-thaw cycles. The solution was cooled to -78 °C in a dry ice/acetone bath, and nitric oxide (43.5 mL, 54 mmHg, 0.124 mmol, 1.2 equiv) was added to the vessel via a volumetric gas bulb. The golden yellow solution changed to dark yellow-green in ~15 minutes. The solution was stirred at -78 °C for 6 hours, then warmed to room temperature. The solvent was removed *in vacuo*, and the residue was washed with THF and filtered through a pad of Celite. The green-yellow solid was extracted with acetonitrile. Vapor diffusion of diethyl ether into an acetonitrile solution of this product yielded crystalline **2** as green urchins,

which were mechanically separated from other precipitates (0.055 g, 27% yield based on [YCu_3]). ^{1}H NMR (CD_3CN, 300 MHz): δ 8.63 (br), 8.42 (br), 7.87 (br overlapped), 7.75 (br overlapped), 7.40 (br), 7.26 (br), 6.88 (br overlapped), 6.72 (br overlapped), 3.6 (br overlapped), 3.35 (br overlapped), 2.09 (br) ppm. ^{19}F NMR (CD_3CN): δ −78.96 ppm. UV-Vis (CH_3CN) λ_{max} [ε ($M^{-1} \times cm^{-1}$)]: 229 nm (1.74×10^5), 369 nm (3.56×10^4), 706 (3.11×10^2). Anal. Calcd. For $C_{144}H_{144}Cu_6F_{18}N_{28}O_{26}S_6Y_2$: C, 45.80; H, 3.84; N, 10.39. Found: C. 46.00; H, 3.91; N, 10.27.

Synthesis of 4.

In a Schlenk tube, a solution of **3** (0.5585 g, 0.927 mmol) in EtCN (8 mL) was degassed by three freeze-pump-thaw cycles. The solution was cooled to -78 °C in a dry ice/acetone bath, and nitric oxide (234 mL, 362 mmHg, 4.64 mmol, 5 equiv.) was added to the vessel via a volumetric gas bulb. The dark yellow solution changed to green-blue in ~1 hour. The solution was stirred at -78 °C for 6 hours, then warmed to room temperature. The solvent was removed *in vacuo*. The residue was triturated with THF and the green solution (which contained mostly desired product) was filtered through a pad of Celite. The material remaining on the Celite filter was extracted with acetonitrile, and the solvent was removed *in vacuo* to give the nitrite product **4** as a green-blue powder (0.369 g, 61%). Single-crystals of **4** suitable for X-ray diffraction studies were obtained via vapor diffusion of diethyl ether into an acetonitrile solution of **4**. ^{1}H NMR (CD_3CN, 300 MHz): δ 9.80 (br), 7.95 (br overlapped), 7.49 (br overlapped), 3.58 (br), 1.14 (br) ppm. ^{19}F NMR (CD_3CN): δ −79.08 ppm. Anal. Calcd. For $C_{26}H_{31}CuF_3N_4O_6S$: C, 48.18; H, 4.82; N, 8.64. Found: C. 48.07; H, 4.74; N, 8.42. Note; addition of 1 equiv. of NO to complex **3** gave a mixture of complex **3** and **4** as judged by ^{1}H NMR spectroscopy (Figure S13).

Synthesis of 5.

In a Schlenk vessel, a solution of **1** (0.3024 g, 0.163 mmol) in 1:1 THF/EtCN was cooled to -78 °C. NO was bubbled through the solution via syringe needle for 1 min, during which the solution turned from yellow to dark green/brown. After stirring at -78 °C for 4 hours, the solution was warmed to room temperature, and precipitation of a brown solid was observed. In the glovebox, the suspension was filtered through Celite, and the brown residue extracted with fresh CH_3CN. The solvent was removed *in vacuo* to give the product as a brown powder (0.241 g, 74%). Single-crystals suitable for X-ray diffraction studies were obtained via vapor diffusion of diethyl ether into an acetonitrile solution of **5**. ^{1}H NMR (CD_3CN, 300 MHz): δ 10.0 (br overlapped), 9.4 (br overlapped), 3.4 (br) ppm. ^{19}F NMR (CD_3CN): δ −78.80 ppm. Anal. Calcd. For $C_{72}H_{72}Cu_3F_9N_{16}O_{18}S_3Y$: C, 43.32; H, 3.64; N, 11.23. Found: C. 43.29; H, 3.76; N, 11.29.

Protocol for Gas Analysis in Reactions of 2 with Acids.

Gas-phase IR: a Schlenk tube was charged with a solution of **2** in CH_3CN. On a Schlenk line, the solution was frozen in LN_2. Under positive N_2 pressure, fresh CH_3CN was layered on top of the frozen solution via syringe and frozen, after

which a CH_3CN solution of pyridinium triflate (6 equiv.) was added and also frozen. The Schlenk tube was sealed, and the solution was thawed and stirred at room temperature for three hours. On a high-vacuum line, N_2 was removed from the solution via three freeze-pump-thaw cycles (the solution was frozen in LN_2 to keep any N_2O produced condensed). The volatiles in the reaction vessel were than vacuum transferred through a trap cooled to -78 °C (to condense CH_3CN) and into a liquid nitrogen-cooled Schlenk flask (to condense N_2O). The flask containing the gaseous products was then connected to an evacuated gas IR cell fitted with two greased joint connections. The gases in the Schlenk flask were allowed to expand into the cell and IR spectra were recorded.

Headspace analysis by GC-MS: in the glovebox, a 10 mL Schlenk flask was charged with a solution of **2** in CH_3CN. On a Schlenk line, the solution was degassed and placed under an argon atmosphere. The solution was frozen in a dry ice/acetone bath. Under positive Ar pressure, fresh CH_3CN sparged with Ar was layered on top of the frozen solution via syringe and frozen, after which a CH_3CN solution of pyridinium triflate (6 equiv.) sparged with Ar was added via syringe and also frozen. The Schlenk tube was sealed with a rubber septum, and the solution was thawed and stirred at room temperature. To analyze the headspace, a gastight microsyringe purged with Ar was used to extract a headspace sample (~5 μL) and inject it into the GC-MS instrument.

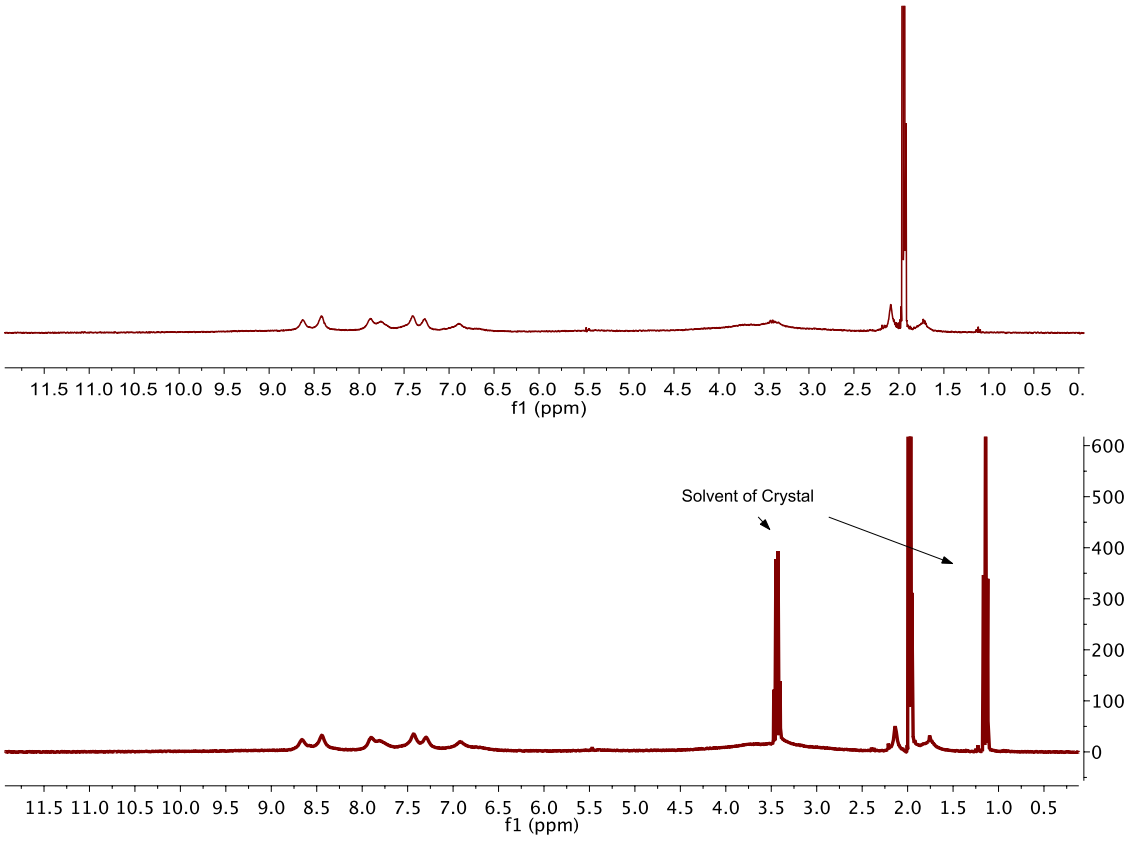

Figure S1. ^1H NMR spectrum of **2** obtained from commercially available nitric oxide (top) and purified nitric oxide (bottom), recorded in CD_3CN.

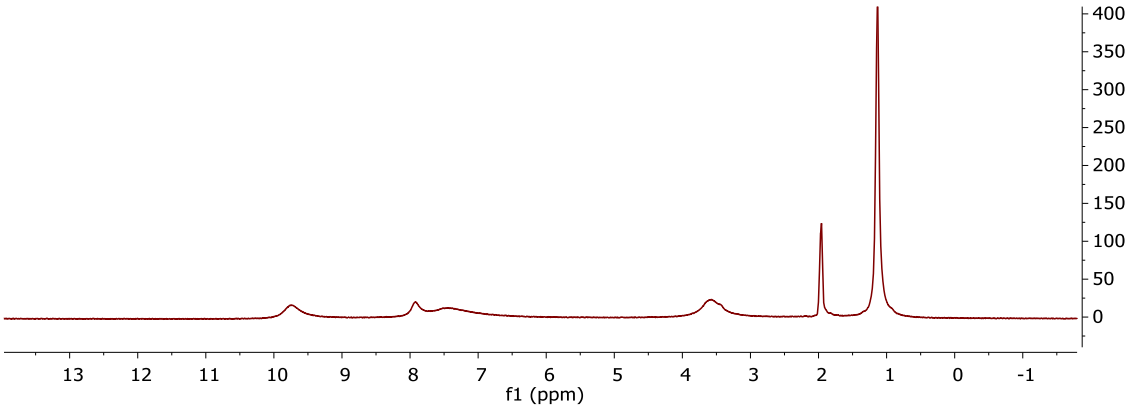

Figure S2. ^{1}H NMR spectrum of **4** in CD_3CN.

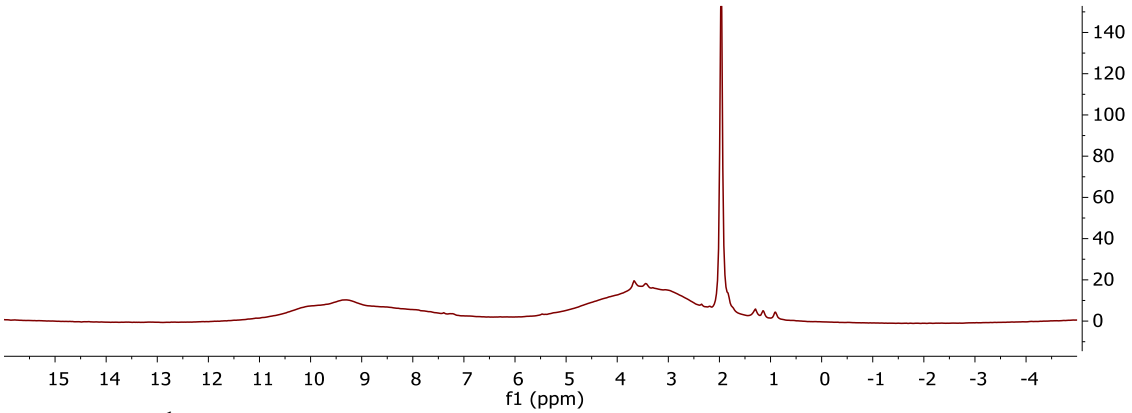

Figure S3. ^{1}H NMR spectrum of **5** in CD_3CN.

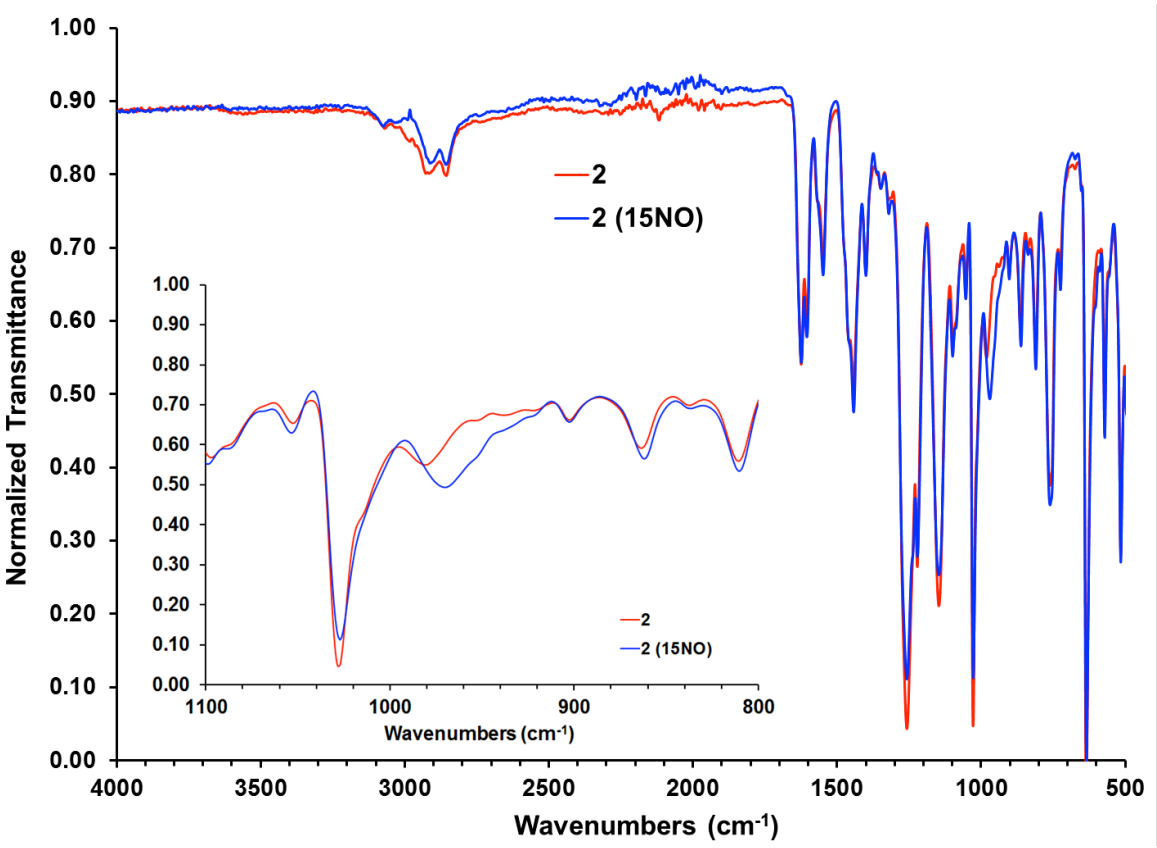

Figure S4. Solid-state ATR-IR spectra of **2** prepared from natural abundance NO (red) and ^{15}NO (blue). The N–O asymmetric stretch region is highlighted in the inset.

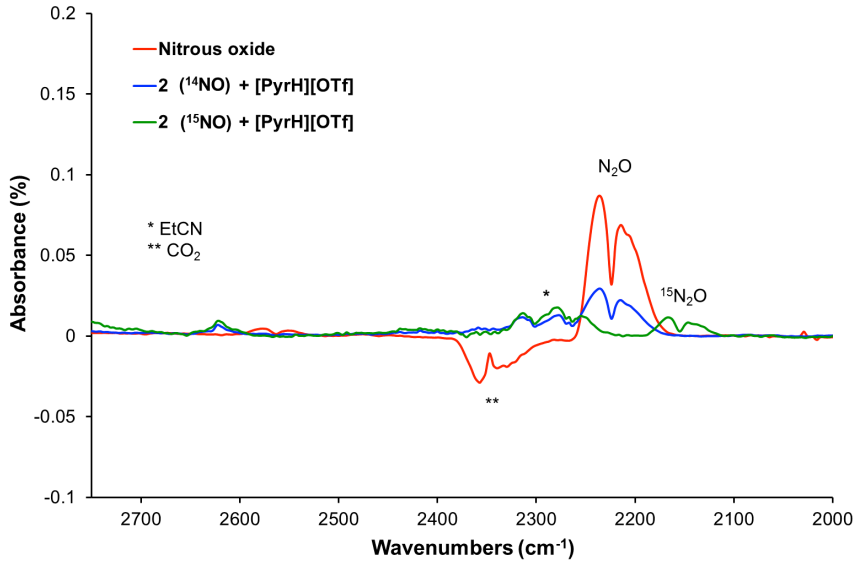

Figure S5. Red: gas-phase IR spectrum of an authentic sample of N_2O. Blue: gas-phase IR spectrum of the products of the reaction of **2** (natural abundance NO) with pyridinium triflate. Green: gas-phase IR spectrum of the products of the reaction of **2** (^{15}NO) with pyridinium triflate.

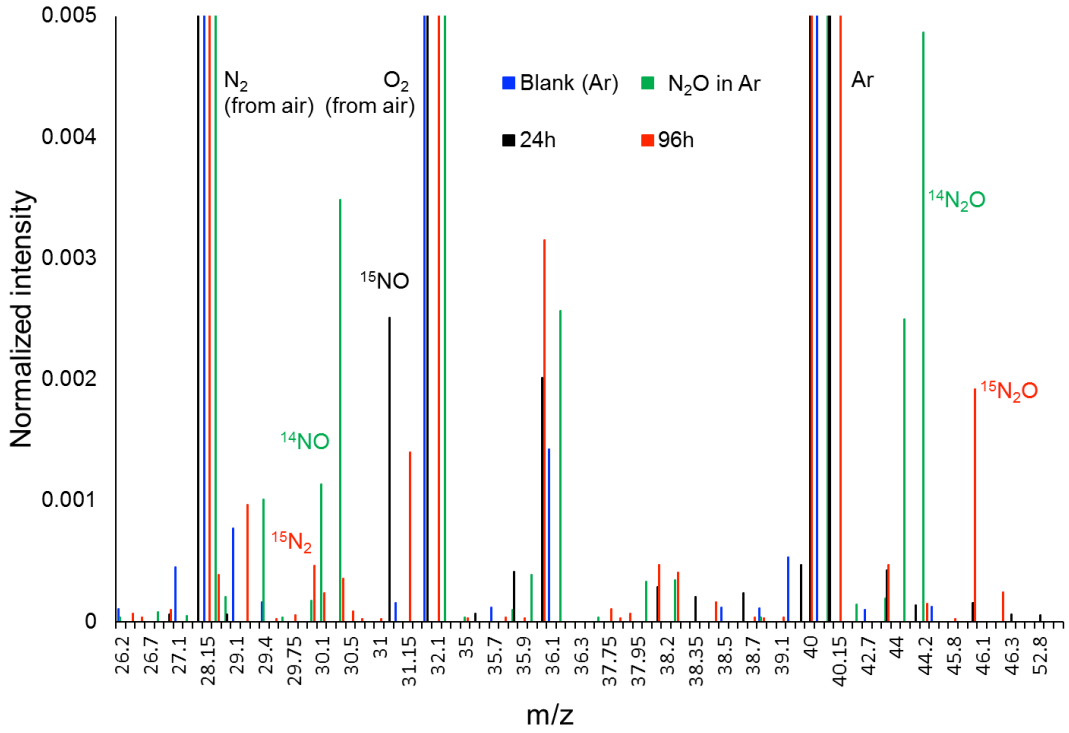

Figure S6. GC-MS data for reactions of ^{15}N-labeled complex **2** with pyridinium triflate at 24 h (black) and 96 h (red). Labels represent assignment of m/z peaks. Peaks at m/z=28 and m/z=32 are due to introduction of air into the GC line during sample injection (as shown by their presence in the Ar blank). Note: peak at m/z=30 (^{14}NO) in authentic $^{14}N_2O$ sample due to fragmentation of N_2O under mass spectrometry conditions. Likewise, the peak at m/z=31 (^{15}NO) observed after 24 h is due to fragmentation of $^{15}N_2O$ under the MS conditions, indicating that release of $^{15}N_2O$ is already occurring at this time point.

Crystallographic Information

Refinement details

Crystals were mounted on a nylon loop using Paratone oil under a nitrogen stream. Low temperature (100 K) X-ray data were obtained on a Bruker APEXII CCD based diffractometer (Mo sealed X-ray tube, K_α = 0.71073 Å). All diffractometer manipulations, including data collection, integration and scaling were carried out using the Bruker APEXII software.[4] Absorption corrections were applied using SADABS.[5] Space groups were determined on the basis of systematic absences and intensity statistics and the structures were solved by direct methods using XS[6] (incorporated into SHELXTL) and refined by full-matrix least squares on F^2. All non-hydrogen atoms were refined using anisotropic displacement parameters. Hydrogen atoms were placed in idealized positions and refined using a riding model. The structures were refined (weighted least squares refinement on F^2) to convergence. It should be noted that due to the size of **2**, its crystal included solvent accessible voids, which tended to contain disordered solvent. These

disordered solvent molecules were largely responsible for the alerts generated by the checkCIF protocol.

Table S1. Crystal and refinement data.

	2	**4**
CCDC #	1425943	1425942
empirical formula	$C_{162}H_{179}Cu_6F_{18}N_{33}O_{28}S_6Y_2$	$C_{26}H_{31}CuF_3N_4O_6S$
formula wt	4129.79	648.15
T (K)	100	100.0
a, Å	13.8507(13)	20.569(2)
b, Å	16.8194(17)	15.5906(15)
c, Å	21.214(2)	18.3755(18)
α, deg	105.556(3)	90
β, deg	105.602(3)	104.318(3)
γ, deg	94.915(3)	90
V, Å^3	4518.7(8)	5709.7(10)
Z	1	8
cryst syst	triclinic	monoclinic
space group	P-1	C2/c
ρ_{calcd}, g/cm^3	1.518	1.508
2θ range, deg	4.384 to 55.028	5.226 to 79.504
μ, mm^{-1}	1.490	0.905
abs corr	Multi-scan	Multi-scan
GOOF[c]	1.038	1.032
R1,[a] wR2[b] (I > 2σ(I))	0.0533, 0.1447	0.0421, 0.1018

[a] $R1 = \Sigma||F_o|-|F_c|| / \Sigma|F_o|$ [b] $wR2 = [\ \Sigma\ [w(F_o^2-F_c^2)^2] / \Sigma\ [w(F_o^2)^2]\ ]^{1/2}$ [c] $GOOF = S = [\ \Sigma\ [w(F_o^2-F_c^2)^2] / (n-p)\ ]^{1/2}$

Special Refinement Details for 2

The structure of **2** displayed disorder in a handful of outer-sphere components. One of the triflate anions was disordered over two positions with ~80:20 occupancy. Due to the considerable size of the complex, large solvent voids existed that required modelling of highly disordered solvent molecules. A diethyl ether molecule was modelled fully (including H atoms) but not refined anisotropically. An acetonitrile molecule residing on a special position was satisfactorily modelled using the EADP and EXYZ commands to account for the disorder of the N atom over two position. H atoms were included but this molecule was also not refined anisotropically.

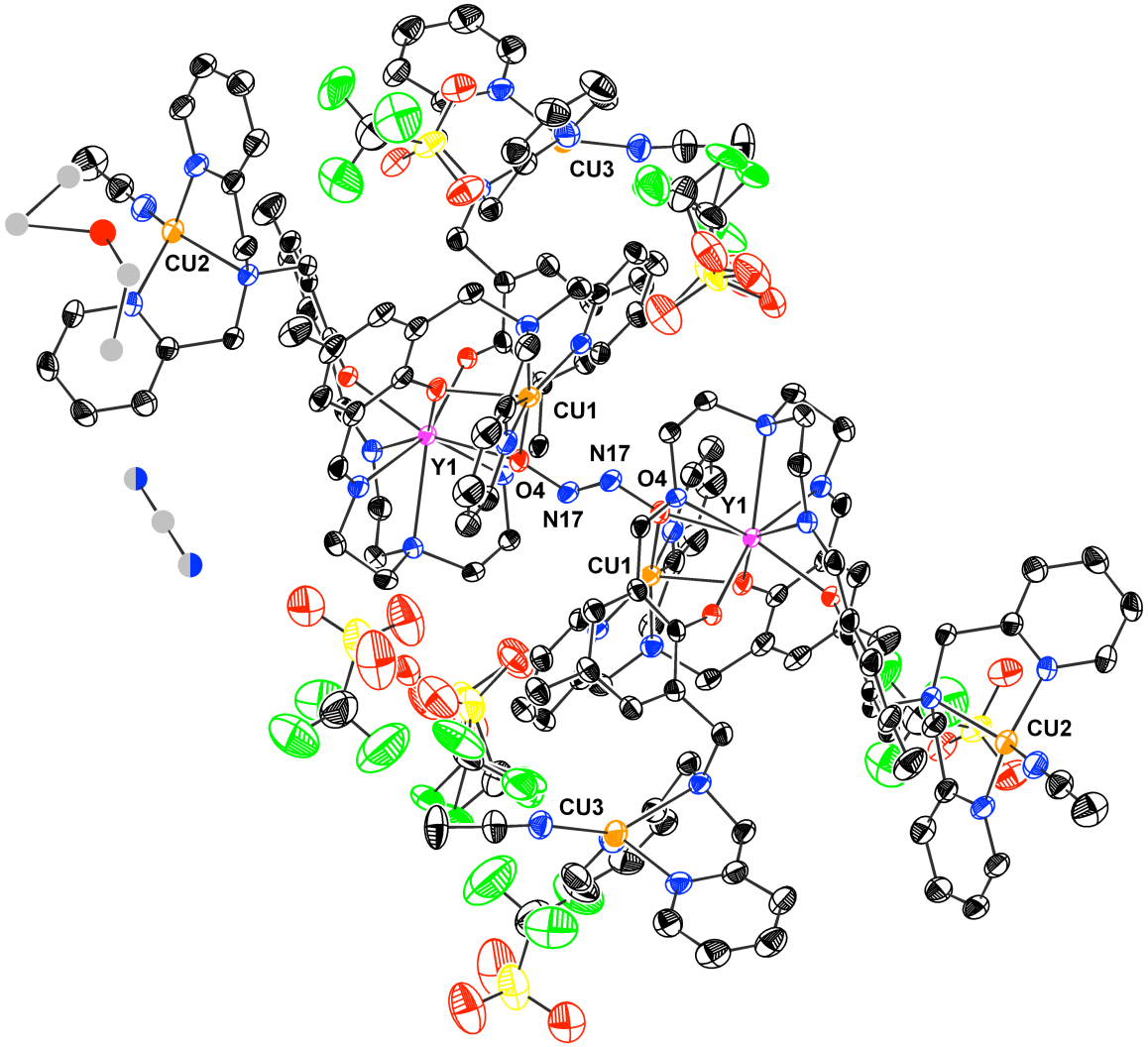

Figure S7. Full solid-state structure of complex **2**. Both components of the disordered outer-sphere triflate moiety are included. Hydrogen atoms omitted for clarity. Thermal ellipsoids shown at the 50% probability level.

Special Refinement Details for 4

The structure of **4** contained disorder at two positions. The outer-sphere triflate anion was disordered over two orientations, which were refined anisotropically as independent parts with 80:20 occupancy. Two disordered outer-sphere solvent molecules were also present that were modeled isotropically, a diethyl ether molecule and an acetonitrile molecule (located at a special position). The disorder in the solvent molecules gave rise to a single A-level alert in the CheckCIF program due to close distances between hydrogen atoms; a comment was included in the .cif file as an explanation for this occurrence.

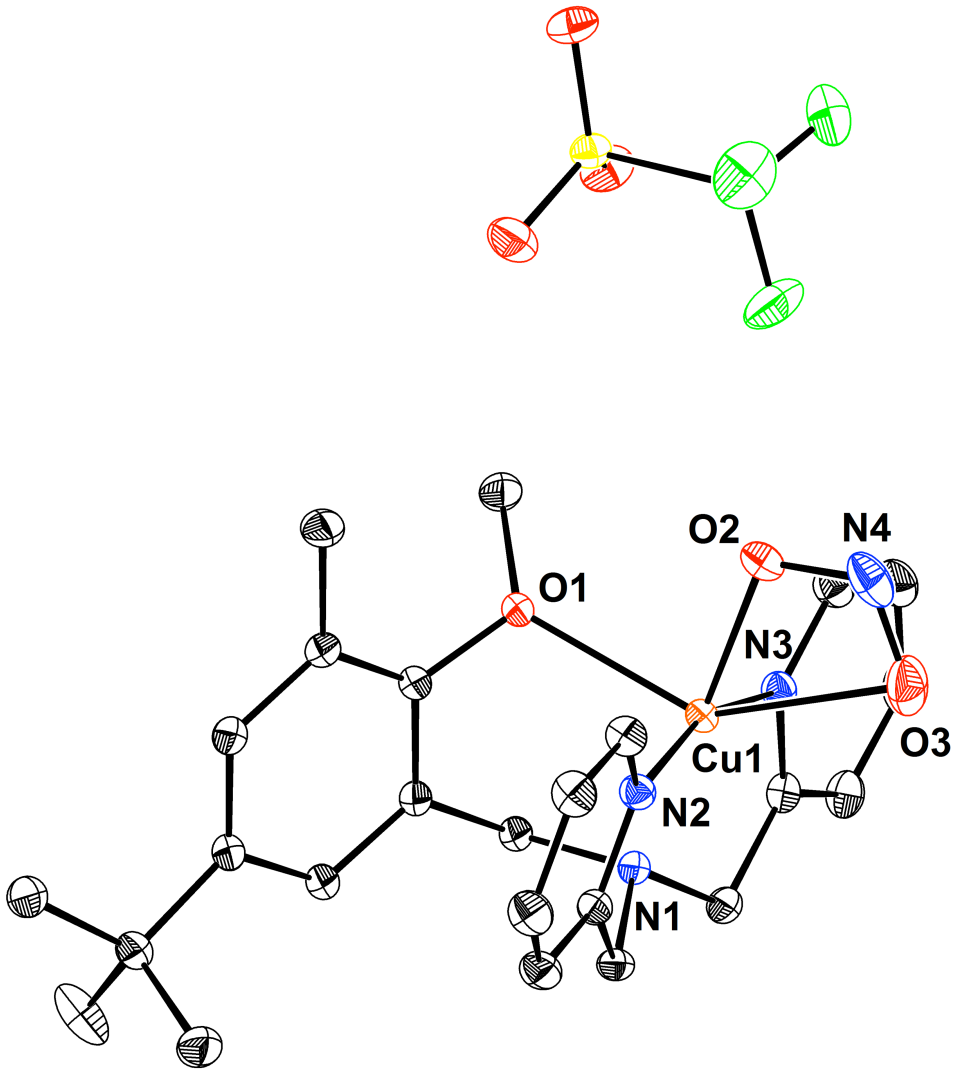

Figure S8. Solid-state structure of complex **4**. Hydrogen atoms omitted for clarity. Thermal ellipsoids shown at the 50% probability level.

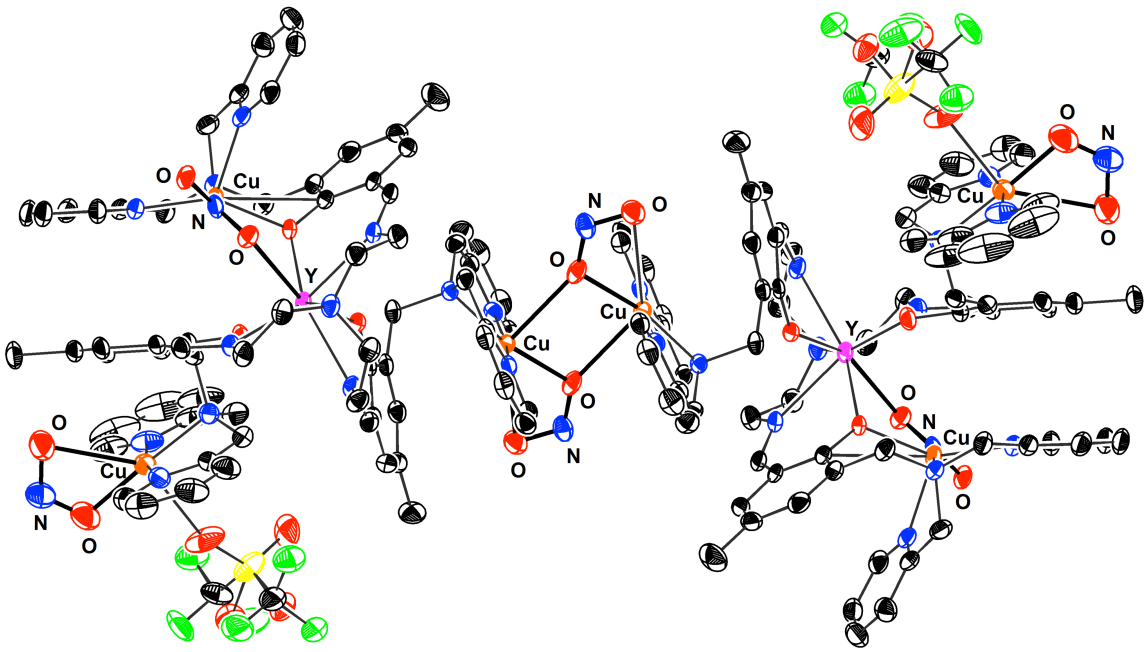

Figure S9. Preliminary solid-state structure of the cationic portion of **5**. Hydrogen atoms, four outer-sphere triflate anions, and outer-sphere solvent molecules omitted for clarity.

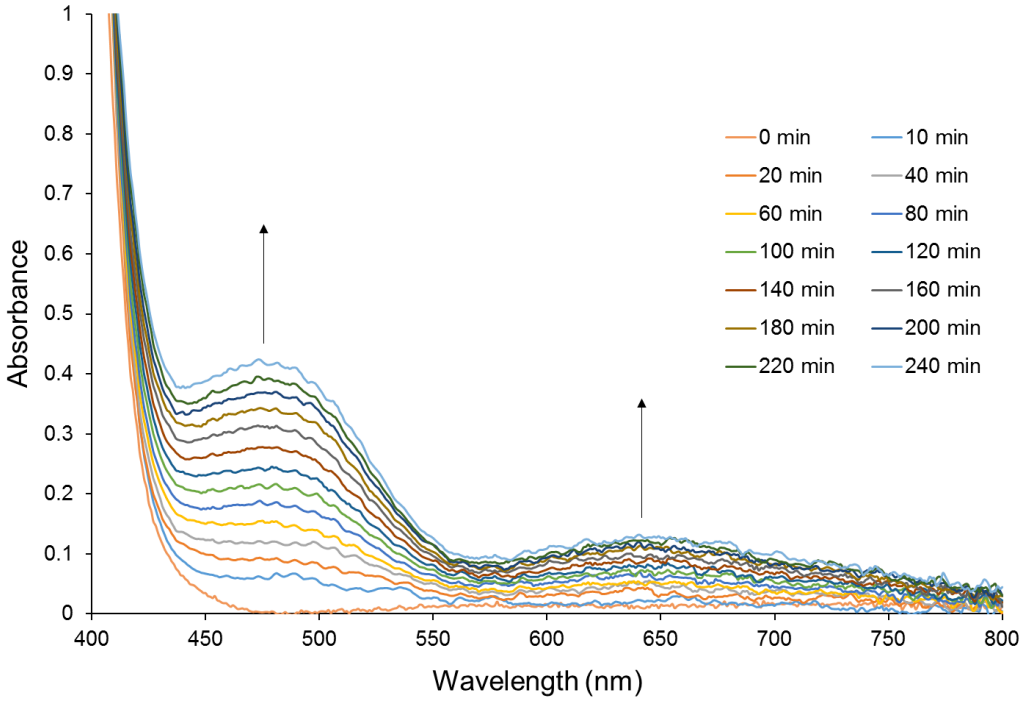

Figure S10. UV-Vis monitoring of the reaction of **1** (0.21 mM in 1:1 EtCN/toluene) with N_2O at -78 °C. The marked features correspond to the $[Cu^{III}Cu^{II}_2(\mu_3\text{-}O)_2]^{3+}$

intermediate.[2]

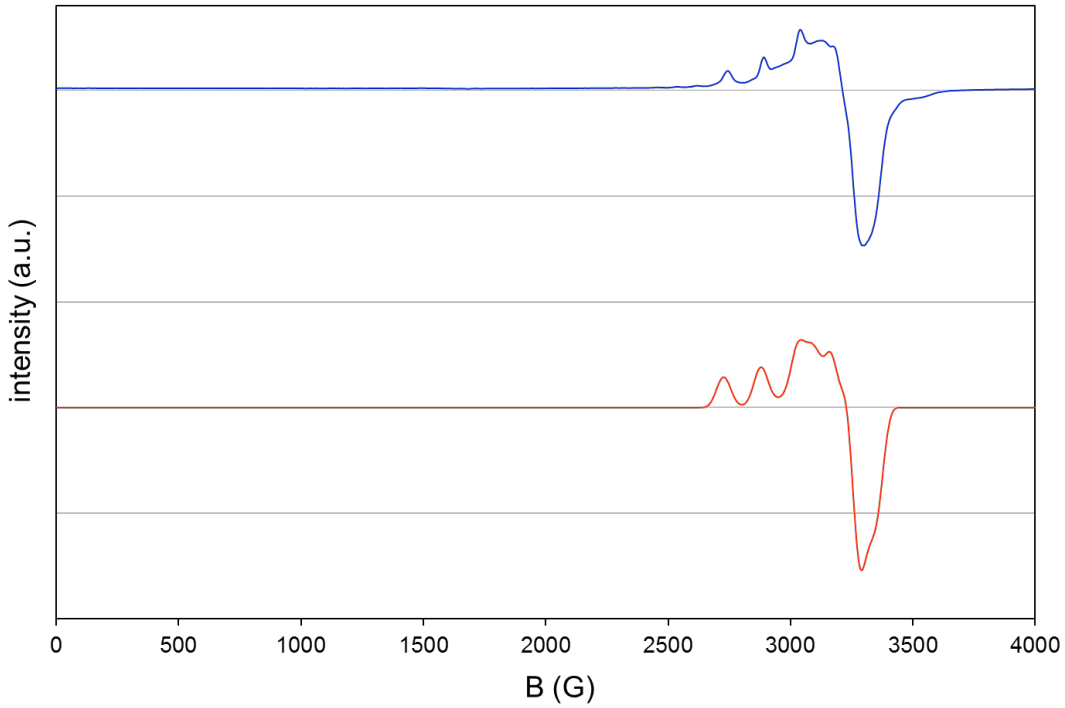

Figure S11. Blue: X-band EPR spectrum of **2** in frozen EtCN at 15K (Frequency: 9.391 GHz; Power: 0.645 mW; Modulation Amplitude: 1 G). Red: EasySpin simulation of EPR data. Simulation parameters: g = [2.05 2.11 2.27]; nuclei: Cu, N, N, N; A = [138 114 475; 50 50 50; 50 50 50; 50 50 50]; HStrain = [95 95 95]; linewidth = 1.

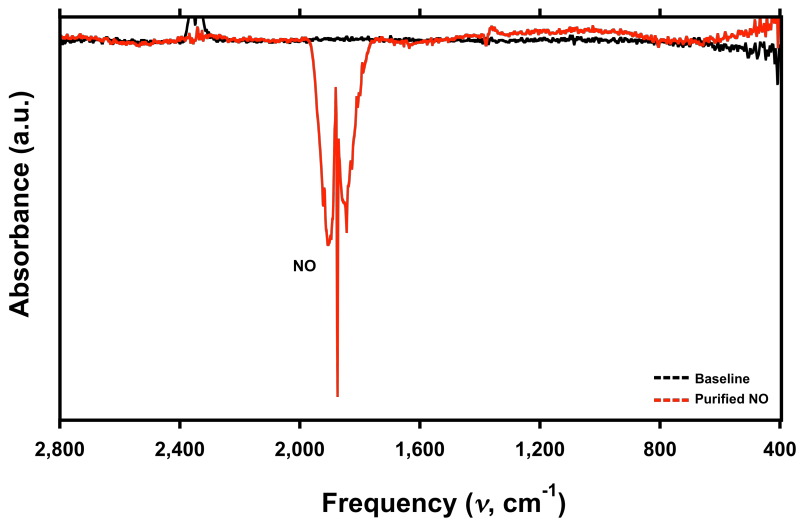

Figure S12. FTIR spectrum of purified nitric (solid red trace). The black trace is the baseline (vacuum).

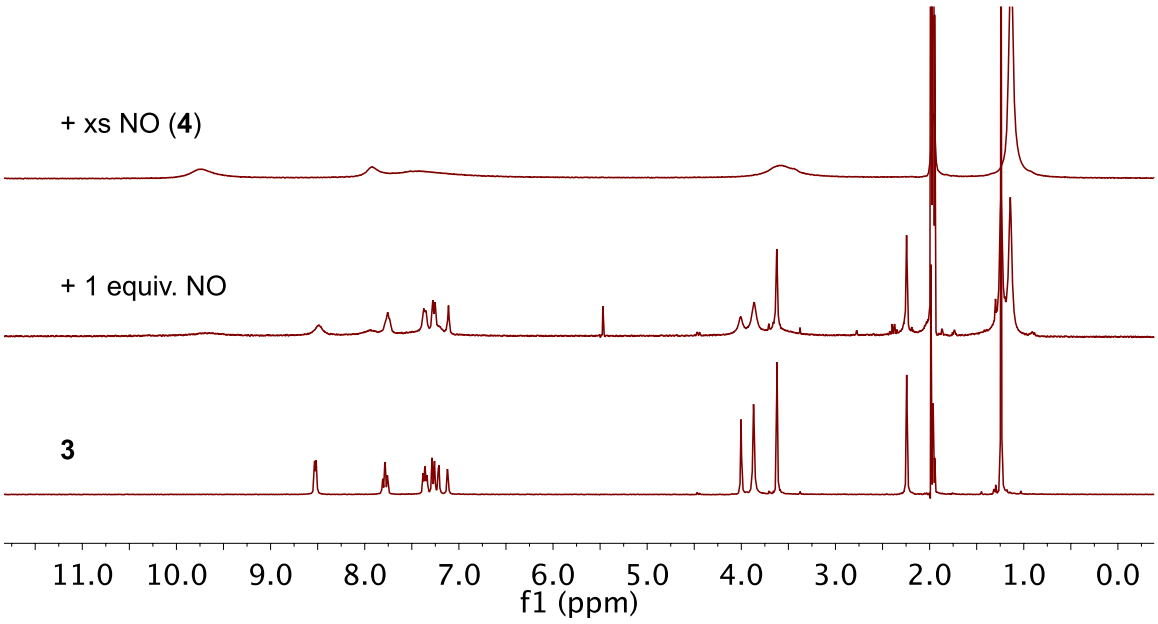

Figure S13. ^{1}H NMR (CD_3CN) spectrum upon addition of 1 equiv. NO (middle) to complex **3**. For comparison the ^{1}H NMR (CD_3CN) of complex **3** (bottom) and complex **4** (top) are shown as well.

Table S2. Fractional Atomic Coordinates ($\times 10^4$) and Equivalent Isotropic Displacement Parameters ($Å^2 \times 10^3$) for 2. U_{eq} is defined as 1/3 of of the trace of the orthogonalised U_{IJ} tensor.

Atom	*x*	*y*	*z*	U(eq)
Y1	4269.0(2)	5066.2(2)	6736.6(2)	20.97(9)
Cu1	5829.4(3)	6364.4(3)	6175.9(2)	22.85(10)
Cu2	4576.0(4)	7375.4(3)	10297.7(2)	30.08(12)
Cu3	1640.1(4)	8728.2(3)	6290.0(2)	34.30(12)
O1	5590.9(18)	6157.5(15)	7094.4(12)	24.7(5)
O2	4246.1(19)	5677.8(15)	7803.0(12)	24.1(5)
O3	3163.0(18)	5895.8(15)	6501.9(12)	23.9(5)
O4	5078.0(19)	5206.9(15)	5842.8(12)	25.9(5)
N1	4285(2)	3450.7(19)	6354.6(15)	26.6(6)
N2	5824(2)	4663(2)	7463.4(15)	28.1(6)
N3	2878(2)	4256.9(19)	6969.2(15)	26.0(6)
N4	3001(2)	4291.2(17)	5565.0(14)	23.7(6)
N5	6540(2)	7576.6(19)	6647.7(15)	25.8(6)
N6	7262(2)	6128(2)	6442.2(15)	29.4(7)
N7	4736(2)	6899.9(18)	5709.3(14)	22.6(6)
N8	5295(2)	7179.3(19)	9465.8(15)	27.5(6)
N9	5467(3)	6525(2)	10520.7(16)	32.2(7)
N10	5249(2)	8572(2)	10488.9(16)	31.1(7)
N11	3301(3)	7212(2)	10469.5(18)	37.6(8)
N12	2440(2)	8064.1(19)	7042.1(15)	26.3(6)
N13	922(3)	9032(2)	7026.4(17)	33.4(7)
N14	3107(3)	9290(2)	6542.4(18)	37.6(8)
N15	864(3)	8554(2)	5354.3(17)	36.5(8)
N17	4792(2)	4794.7(19)	5148.0(15)	27.1(6)
C1	5306(3)	3261(2)	6660.7(19)	31.4(8)
C2	5740(3)	3773(2)	7413.0(19)	33.5(8)
C3	3522(3)	2975(2)	6553(2)	30.3(8)
C4	2573(3)	3370(2)	6568(2)	30.7(8)
C5	4085(3)	3201(2)	5599.5(18)	29.5(8)
C6	3116(3)	3431(2)	5217.7(18)	29.7(8)
C7	6630(3)	5133(3)	7900.4(18)	30.8(8)
C8	6915(3)	6027(2)	8045.2(18)	28.7(8)
C9	7792(3)	6436(3)	8604.5(19)	33.1(9)
C10	8153(3)	7275(3)	8783.3(19)	37.1(10)
C11	7654(3)	7724(3)	8363.6(19)	33.3(9)
C12	6810(3)	7347(2)	7800.3(18)	28.6(8)
C13	6395(3)	6494(2)	7637.2(17)	25.6(7)
C14	9065(3)	7714(3)	9400(2)	48.2(12)

C15	6331(3)	7830(2)	7333.3(18)	28.6(8)
C16	7653(3)	7643(3)	6747(2)	32.2(8)
C17	7983(3)	6821(3)	6740.4(18)	32.8(8)
C18	9006(3)	6772(3)	7002(2)	47.1(11)
C19	9266(4)	5990(4)	6954(2)	54.5(13)
C20	8532(4)	5289(3)	6671(2)	46.5(11)
C21	7527(3)	5377(3)	6420(2)	36.2(9)
C22	6085(3)	8106(2)	6228.9(19)	28.3(8)
C23	5000(3)	7729(2)	5816.6(18)	25.5(7)
C24	4328(3)	8184(2)	5514.9(19)	29.6(8)
C25	3369(3)	7782(2)	5091(2)	31.4(8)
C26	3102(3)	6932(2)	4985.0(19)	28.8(8)
C27	3794(3)	6515(2)	5302.5(17)	24.2(7)
C28	2312(3)	4574(2)	7329.7(18)	28.7(8)
C29	2517(3)	5415(2)	7791.5(18)	27.9(8)
C30	1745(3)	5699(3)	8065.0(19)	35.1(9)
C31	1887(3)	6484(3)	8540(2)	39.1(10)
C32	2850(3)	6972(3)	8763.9(19)	34.9(9)
C33	3646(3)	6714(2)	8529.6(17)	26.9(8)
C34	3496(3)	5926(2)	8021.6(17)	25.5(7)
C35	1035(4)	6794(4)	8807(3)	57.1(14)
C36	4671(3)	7269(2)	8803.7(17)	28.7(8)
C37	6204(3)	7841(2)	9784(2)	32.5(8)
C38	5950(3)	8652(2)	10168.7(18)	30.1(8)
C39	6447(3)	9426(3)	10210(2)	36.8(9)
C40	6212(3)	10148(3)	10603(2)	38.7(9)
C41	5489(3)	10065(3)	10931(2)	38.5(9)
C42	5023(3)	9273(3)	10862(2)	35.4(9)
C43	5601(3)	6351(2)	9371.5(18)	30.8(8)
C44	5830(3)	6108(2)	10024.8(18)	30.1(8)
C45	6348(3)	5448(3)	10092(2)	37.1(9)
C46	6474(4)	5197(3)	10675(2)	43.5(10)
C47	6095(4)	5636(3)	11188(2)	43(1)
C48	5614(4)	6285(3)	11093(2)	40.1(10)
C49	2616(4)	7206(3)	10680(2)	41.5(10)
C50	1759(4)	7204(4)	10948(3)	60.4(14)
C51	2263(3)	4557(2)	5212.0(17)	24.1(7)
C52	1893(3)	5336(2)	5409.0(17)	22.4(7)
C53	1061(3)	5470(2)	4926.2(18)	25.9(7)
C54	612(3)	6172(2)	5062.9(19)	26.8(7)
C55	950(3)	6704(2)	5732.6(19)	28.9(8)
C56	1769(3)	6609(2)	6234.1(18)	26.1(7)

C57	2321(3)	5943(2)	6069.6(17)	23.1(7)
C58	-216(3)	6340(3)	4511(2)	34.0(8)
C59	2035(3)	7181(2)	6959.5(19)	30.3(8)
C60	3496(3)	8152(2)	7026(2)	31.0(8)
C61	3826(3)	9003(3)	6958(2)	34.5(9)
C62	4797(3)	9457(3)	7281(2)	39.7(9)
C63	5074(4)	10181(3)	7136(3)	50.1(12)
C64	4358(4)	10441(3)	6677(3)	58.5(14)
C65	3382(4)	9999(3)	6408(3)	47.9(11)
C66	2379(3)	8610(3)	7696.2(19)	34.3(9)
C67	1349(3)	8873(3)	7616(2)	33.5(8)
C68	909(3)	9003(3)	8145(2)	40.7(10)
C69	18(4)	9332(3)	8065(3)	48.6(11)
C70	-416(3)	9506(3)	7462(3)	49.5(12)
C71	53(3)	9342(3)	6949(2)	41.5(10)
C72	408(3)	8551(3)	4822(2)	38.8(9)
C73	-186(4)	8521(4)	4137(2)	56.9(14)
O17	7885(14)	8229(11)	11581(9)	298(7)
C78	7730(20)	8073(17)	12457(15)	355(15)
C79	7111(13)	8674(11)	12048(8)	191(6)
C80	8940(30)	8040(30)	11320(20)	530(30)
C81	9010(30)	6970(20)	11145(17)	412(19)
S2	8524.6(14)	3359.0(14)	7213.6(9)	79.7(5)
F4	8873(5)	1974(4)	7484(3)	138(2)
F5	7317(4)	2038(3)	7098(3)	117.9(16)
F6	8223(5)	1826(5)	6421(3)	157(3)
O8	9498(4)	3450(5)	7131(3)	117(2)
O9	7717(4)	3517(4)	6702(3)	99.1(17)
O10	8472(4)	3697(3)	7900(3)	90.5(14)
C75	8206(7)	2244(5)	7040(4)	89(2)
S3	7619(15)	9226(13)	5303(11)	60(5)
F7	7020(50)	9938(18)	6150(30)	91(17)
F8	8272(17)	10438(11)	6363(9)	83(7)
F9	7110(20)	10660(12)	5549(15)	75(7)
O11	6611(18)	8868(12)	4758(12)	80(9)
O13	8000(70)	8570(40)	5600(40)	58(18)
O15	8287(19)	9467(17)	4956(15)	79(9)
C76	7440(40)	10130(30)	5880(20)	73(10)
S4	7888(3)	9180(2)	5232.0(19)	34.0(7)
F10	6843(13)	9956(7)	6023(8)	110(5)
F11	5953(3)	9198(3)	5039(3)	84.9(18)
F12	6812(5)	10384(3)	5160(3)	61.0(13)

O12	8773(3)	9818(3)	5573(3)	64.1(16)
O14	7808(16)	8528(8)	5550(8)	38(2)
O16	7641(4)	8904(3)	4500(2)	53.6(13)
C77	6843(6)	9713(4)	5383(4)	54.0(18)
S1	7393.8(8)	10155.5(7)	8633.5(5)	38.5(2)
F1	8805(3)	9877(3)	9608(2)	95.3(13)
F2	8089(3)	10927(2)	9954.4(17)	91.7(13)
F3	9174(3)	11021(3)	9396(2)	99.8(14)
O5	7874(3)	9752(2)	8146.6(18)	53.2(9)
O6	7060(3)	10915(2)	8546.8(18)	51.4(8)
O7	6677(2)	9588.7(19)	8763.0(15)	41.3(7)
C74	8410(5)	10514(4)	9436(3)	64.9(15)
C82	10000	5000	10000	282(16)
N16	9380(20)	5337(17)	10365(13)	335(12)
C83	9380(20)	5337(17)	10365(13)	335(12)

Table S3. Anisotropic Displacement Parameters ($Å^2 \times 10^3$) for 2. The Anisotropic displacement factor exponent takes the form: $-2\pi^2[h^2a^{*2}U_{11}+2hka^*b^*U_{12}+\ldots]$.

Atom	U_{11}	U_{22}	U_{33}	U_{23}	U_{13}	U_{12}
Y1	26.05(17)	21.47(16)	13.72(15)	3.99(12)	3.76(12)	7.08(13)
Cu1	26.3(2)	21.1(2)	17.9(2)	2.35(16)	4.69(16)	4.84(16)
Cu2	36.9(3)	32.7(2)	22.8(2)	7.91(18)	11.66(19)	10.5(2)
Cu3	38.3(3)	38.2(3)	22.7(2)	8.4(2)	2.68(19)	11.4(2)
O1	25.6(12)	29.0(13)	15.4(11)	3.4(9)	3.3(9)	3.9(10)
O2	29.9(13)	24.7(12)	16.9(11)	5.1(9)	5.6(10)	8.8(10)
O3	28.6(13)	23.4(12)	16.4(11)	5.1(9)	1.5(9)	6.6(10)
O4	34.8(14)	22.3(12)	14.9(11)	3.5(9)	1.8(10)	1.2(10)
N1	33.6(16)	26.1(15)	19.8(14)	7.9(12)	5.0(12)	11.0(13)
N2	32.9(16)	31.2(16)	20.3(14)	7.1(12)	6.9(13)	13.2(13)
N3	30.4(16)	26.3(15)	19.7(14)	7.0(12)	4.3(12)	7.1(12)
N4	31.5(16)	17.6(14)	18.7(14)	2.9(11)	5.2(12)	4.0(12)
N5	24.8(15)	25.4(15)	22.6(15)	3.7(12)	3.6(12)	3.1(12)
N6	32.8(16)	36.6(17)	20.2(14)	7.8(13)	9.6(13)	12.1(14)
N7	26.0(15)	20.5(14)	19.0(13)	2.6(11)	7.4(11)	1.8(11)
N8	36.6(17)	27.0(15)	18.2(14)	4.8(12)	7.6(12)	10.1(13)
N9	43.4(19)	32.0(17)	19.6(15)	7.9(13)	5.9(13)	10.0(14)
N10	35.1(17)	31.5(17)	24.3(15)	3.1(13)	9.8(13)	8.6(14)
N11	44(2)	38.6(19)	30.2(17)	7.8(15)	14.0(15)	5.7(16)
N12	27.6(15)	27.3(15)	20.8(14)	3.7(12)	4.7(12)	7.9(12)
N13	32.9(17)	32.4(17)	29.0(16)	3.4(13)	3.9(13)	12.7(14)

N14	39.0(19)	37.8(19)	33.8(18)	11.6(15)	6.3(15)	8.4(15)
N15	39.2(19)	39.0(19)	28.0(17)	9.6(14)	6.1(15)	3.8(15)
N17	31.9(16)	26.9(16)	18.4(14)	2.4(11)	4.9(12)	7.2(13)
C1	39(2)	27.6(19)	29.3(19)	8.7(15)	9.3(16)	16.3(16)
C2	40(2)	36(2)	25.4(18)	13.6(16)	3.4(16)	14.9(17)
C3	40(2)	25.7(18)	28.8(19)	13.2(15)	10.2(16)	9.9(16)
C4	35(2)	26.9(19)	28.8(19)	8.7(15)	7.7(16)	2.2(15)
C5	42(2)	21.3(17)	22.2(17)	2.3(14)	8.4(15)	8.6(15)
C6	44(2)	20.6(17)	19.2(17)	1.9(13)	5.0(15)	4.7(15)
C7	34(2)	43(2)	17.7(16)	9.7(15)	6.1(15)	18.7(17)
C8	25.7(18)	40(2)	17.4(16)	3.7(15)	5.9(14)	11.3(15)
C9	29.9(19)	46(2)	19.1(17)	4.1(16)	3.6(15)	14.3(17)
C10	25.6(19)	55(3)	19.6(18)	-3.5(17)	2.7(15)	11.1(18)
C11	30.1(19)	36(2)	24.6(18)	-5.2(15)	8.0(15)	3.8(16)
C12	26.3(18)	34(2)	19.4(16)	-0.3(14)	6.2(14)	6.4(15)
C13	24.8(17)	31.5(19)	18.1(16)	1.7(14)	7.9(13)	7.1(14)
C14	32(2)	57(3)	33(2)	-7(2)	-5.7(18)	9(2)
C15	27.5(18)	25.4(18)	25.9(18)	-1.2(14)	6.3(15)	2.8(14)
C16	25.8(18)	38(2)	26.9(19)	4.6(16)	5.1(15)	0.9(16)
C17	32(2)	45(2)	17.1(16)	5.9(16)	3.9(14)	9.1(17)
C18	33(2)	64(3)	34(2)	7(2)	-0.6(18)	15(2)
C19	42(3)	73(4)	38(2)	10(2)	-2(2)	28(3)
C20	60(3)	52(3)	34(2)	16(2)	15(2)	33(2)
C21	46(2)	42(2)	26.4(19)	11.9(17)	13.7(17)	19.4(19)
C22	29.9(19)	20.8(17)	29.3(18)	5.4(14)	4.9(15)	-0.6(14)
C23	30.4(18)	21.4(17)	22.5(17)	3.1(13)	9.1(14)	1.9(14)
C24	37(2)	22.5(17)	29.6(19)	10.0(15)	8.4(16)	3.9(15)
C25	30.3(19)	32(2)	34(2)	15.5(16)	7.5(16)	8.4(16)
C26	25.8(18)	31.2(19)	28.2(18)	12.4(15)	3.9(15)	1.8(15)
C27	29.7(18)	21.5(16)	20.0(16)	5.7(13)	7.2(14)	-0.2(14)
C28	26.5(18)	37(2)	23.1(17)	13.2(15)	2.6(14)	9.1(15)
C29	30.7(19)	36(2)	18.5(16)	10.2(15)	5.7(14)	13.5(16)
C30	33(2)	49(2)	24.4(18)	12.6(17)	6.2(16)	16.5(18)
C31	42(2)	57(3)	21.3(18)	9.1(18)	11.0(17)	27(2)
C32	49(2)	38(2)	17.6(17)	7.2(15)	6.8(16)	24.4(19)
C33	40(2)	28.3(18)	14.2(15)	8.0(13)	6.6(14)	16.1(16)
C34	34.6(19)	29.5(18)	16.0(15)	11.3(14)	6.4(14)	14.9(15)
C35	44(3)	82(4)	39(3)	3(2)	13(2)	30(3)
C36	46(2)	25.3(18)	17.7(16)	8.0(14)	10.6(15)	14.3(16)
C37	35(2)	36(2)	26.8(19)	5.7(16)	14.2(16)	8.5(17)
C38	32.6(19)	32(2)	21.6(17)	3.2(15)	6.8(15)	5.6(16)
C39	39(2)	39(2)	29(2)	6.1(17)	10.3(17)	1.7(18)

C40	44(2)	30(2)	32(2)	2.6(17)	3.7(18)	1.5(17)
C41	48(2)	33(2)	27(2)	1.4(16)	5.9(18)	10.1(18)
C42	40(2)	38(2)	25.3(19)	2.2(16)	10.8(16)	11.2(18)
C43	42(2)	31.4(19)	19.3(17)	6.7(15)	7.9(15)	14.6(16)
C44	34(2)	29.6(19)	21.4(17)	5.2(14)	2.3(15)	8.3(15)
C45	39(2)	39(2)	32(2)	10.6(17)	6.0(17)	12.5(18)
C46	50(3)	42(2)	38(2)	17.4(19)	2.8(19)	19(2)
C47	57(3)	43(2)	22.3(19)	12.6(17)	-1.8(18)	11(2)
C48	55(3)	42(2)	20.8(18)	8.7(17)	8.4(18)	12(2)
C49	46(3)	39(2)	36(2)	7.8(18)	13(2)	1.4(19)
C50	56(3)	60(3)	70(4)	14(3)	36(3)	0(3)
C51	28.3(18)	22.9(17)	15.8(15)	2.8(13)	3.2(13)	-2.0(14)
C52	23.2(16)	21.8(16)	21.7(16)	9.0(13)	4.3(13)	0.9(13)
C53	26.4(17)	24.1(17)	22.5(17)	7.0(14)	1.2(14)	-1.1(14)
C54	22.3(17)	27.3(18)	29.7(18)	13.4(15)	2.6(14)	0.7(14)
C55	30.5(19)	28.5(18)	29.5(19)	12.7(15)	7.6(15)	7.6(15)
C56	30.7(18)	24.4(17)	22.0(17)	7.5(14)	5.2(14)	6.2(14)
C57	26.5(17)	24.5(17)	18.1(15)	8.9(13)	3.8(13)	4.6(14)
C58	28.8(19)	35(2)	34(2)	16.0(17)	-0.5(16)	2.1(16)
C59	35(2)	35(2)	24.7(18)	12.3(15)	10.4(15)	15.2(16)
C60	31.5(19)	34(2)	26.4(18)	7.5(15)	7.9(15)	11.0(16)
C61	40(2)	35(2)	27.5(19)	7.8(16)	8.6(16)	12.4(17)
C62	40(2)	38(2)	34(2)	5.2(18)	6.2(18)	5.8(18)
C63	47(3)	34(2)	58(3)	6(2)	8(2)	-1(2)
C64	61(3)	35(2)	76(4)	23(2)	10(3)	3(2)
C65	55(3)	39(2)	53(3)	22(2)	12(2)	14(2)
C66	38(2)	39(2)	22.0(18)	4.1(16)	5.8(16)	14.0(17)
C67	34(2)	35(2)	27.9(19)	3.2(16)	7.3(16)	12.6(17)
C68	37(2)	52(3)	29(2)	4.5(18)	9.2(17)	15.1(19)
C69	40(2)	61(3)	45(3)	6(2)	20(2)	17(2)
C70	34(2)	56(3)	57(3)	11(2)	14(2)	19(2)
C71	34(2)	46(3)	41(2)	13(2)	5.2(18)	13.0(19)
C72	32(2)	48(2)	33(2)	15.9(19)	4.9(17)	-3.7(18)
C73	46(3)	83(4)	33(2)	26(2)	-3(2)	-14(3)
S2	73.7(10)	113.6(15)	72.5(11)	54.9(10)	25.8(9)	27.2(10)
F4	158(5)	130(4)	154(5)	75(4)	44(4)	86(4)
F5	120(4)	89(3)	137(5)	24(3)	37(4)	22(3)
F6	176(6)	185(6)	99(4)	-3(4)	56(4)	72(5)
O8	69(3)	206(7)	120(5)	98(5)	42(3)	47(4)
O9	78(3)	136(5)	97(4)	71(4)	11(3)	24(3)
O10	113(4)	84(3)	74(3)	28(3)	24(3)	20(3)
C75	101(6)	107(6)	67(4)	22(4)	32(4)	55(5)

S3	80(11)	63(6)	53(5)	32(4)	31(6)	19(6)
F7	200(40)	13(10)	52(14)	12(10)	21(18)	25(14)
F8	110(16)	62(11)	57(11)	21(8)	-6(10)	-4(10)
F9	112(18)	22(9)	103(18)	30(11)	38(16)	18(10)
O11	71(15)	50(11)	80(15)	22(10)	-33(12)	-24(10)
O13	22(18)	70(30)	80(30)	40(20)	4(13)	3(13)
O15	80(17)	95(18)	120(30)	80(20)	73(19)	40(15)
C76	100(30)	80(20)	60(20)	30(20)	50(20)	30(20)
S4	42.0(13)	24.2(9)	32.5(12)	12.7(8)	3.9(10)	-1.0(9)
F10	213(12)	80(6)	108(9)	61(5)	112(10)	83(7)
F11	44(2)	64(3)	174(5)	71(3)	41(3)	17(2)
F12	93(4)	34(3)	75(3)	30(2)	38(3)	23(2)
O12	49(3)	51(3)	78(4)	36(3)	-11(2)	-20(2)
O14	41(8)	27(4)	51(4)	22(3)	13(4)	2(3)
O16	74(3)	45(3)	39(2)	18(2)	7(2)	14(2)
C77	81(5)	33(3)	68(5)	30(3)	39(4)	20(3)
S1	32.6(5)	38.5(5)	33.9(5)	-3.8(4)	8.8(4)	2.9(4)
F1	71(2)	93(3)	89(3)	28(2)	-27(2)	6(2)
F2	121(3)	80(2)	36.8(17)	-13.6(16)	3.9(19)	-15(2)
F3	64(2)	96(3)	94(3)	10(2)	-17(2)	-37(2)
O5	47.6(19)	48.3(19)	59(2)	-1.6(16)	27.6(17)	0.8(15)
O6	51.4(19)	42.6(18)	54(2)	5.2(15)	14.9(16)	7.2(15)
O7	39.2(16)	44.9(17)	33.9(15)	1.1(13)	13.4(13)	3.7(13)
C74	59(3)	60(3)	49(3)	2(3)	-7(3)	-7(3)

Table S4. Fractional Atomic Coordinates ($\times 10^4$) and Equivalent Isotropic Displacement Parameters ($Å^2 \times 10^3$) for 4. U_{eq} is defined as 1/3 of of the trace of the orthogonalised U_{IJ} tensor.

Atom	***x***	***y***	***z***	**U(eq)**
Cu01	5884.0(2)	3541.6(2)	3976.3(2)	13.49(3)
O1	6614.3(4)	3906.4(6)	5120.6(5)	18.56(15)
O2	5193.5(5)	3502.8(6)	4563.3(6)	20.67(16)
O3	4635.8(6)	3351.2(8)	3443.9(7)	34.5(3)
N1	6625.3(5)	3559.8(6)	3430.2(5)	13.85(14)
N2	5798.3(5)	4771.9(6)	3713.4(6)	16.01(16)
N3	6014.0(5)	2286.0(7)	3938.3(6)	16.56(16)
N4	4614.8(6)	3397.0(9)	4108.7(9)	29.9(3)
C1	7092.9(5)	4513.9(7)	5049.2(6)	15.62(17)
C2	7411.5(5)	4375.3(7)	4469.6(6)	15.11(17)
C3	7838.7(6)	5004.2(8)	4312.2(6)	16.28(18)
C4	7959.2(6)	5767.0(7)	4725.7(6)	16.44(18)

C5	7643.8(6)	5872.2(8)	5308.0(6)	18.25(19)
C6	7200.9(6)	5262.0(8)	5475.9(6)	17.10(18)
C7	8386.4(6)	6470.6(8)	4492.3(7)	18.89(19)
C8	7981.6(8)	6858.2(10)	3747.6(8)	27.7(3)
C9	9043.5(8)	6111.2(11)	4373.8(12)	36.7(4)
C10	8557.3(8)	7192(1)	5075.9(8)	28.6(3)
C11	6847.5(7)	5438.7(9)	6086.4(7)	23.3(2)
C12	7289.0(5)	3567.8(7)	4008.1(6)	15.08(16)
C13	6539.6(6)	4334.0(7)	2940.3(6)	16.45(18)
C14	6175.4(6)	5031.7(7)	3250.8(6)	16.23(17)
C15	6197.7(7)	5889.1(8)	3049.5(7)	21.2(2)
C16	5821.9(7)	6485.7(8)	3329.3(8)	23.5(2)
C17	5436.0(7)	6213.2(8)	3810.2(8)	23.0(2)
C18	5440.6(6)	5354.4(8)	3991.8(7)	19.3(2)
C19	6572.4(6)	2748.1(7)	2993.2(6)	16.70(18)
C20	6338.9(6)	2033.7(7)	3421.1(6)	16.68(18)
C21	6414.9(6)	1172.0(8)	3268.3(7)	21.0(2)
C22	6151.3(7)	555.5(8)	3659.6(8)	24.1(2)
C23	5826.5(7)	818.9(8)	4199.8(8)	24.4(2)
C24	5767.5(6)	1687.0(8)	4326.3(7)	20.2(2)
C25	6712.2(7)	3446.9(8)	5815.8(7)	21.8(2)
S1	6485.2(2)	1423.5(2)	7403.4(2)	17.75(5)
F1	5284.4(5)	1971.1(8)	6711.2(7)	42.3(3)
F2	5775.9(6)	1226.4(8)	6012.6(5)	40.7(2)
F3	5357.7(5)	599.6(7)	6836.2(7)	40.0(2)
O4	6289.6(6)	1498.4(6)	8101.5(5)	23.83(18)
O5	6758.9(6)	2193.0(7)	7157.3(7)	31.3(2)
O6	6837.0(5)	639.8(7)	7317.5(6)	26.7(2)
C26	5681.7(7)	1297.3(10)	6708.9(8)	25.1(2)

Table S5. Anisotropic Displacement Parameters ($Å^2 \times 10^3$) for 4. The Anisotropic displacement factor exponent takes the form: $-2\pi^2[h^2a^{*2}U_{11}+2hka^*b^*U_{12}+\ldots]$.

Atom	U_{11}	U_{22}	U_{33}	U_{23}	U_{13}	U_{12}
Cu01	13.00(6)	13.03(6)	14.68(6)	0.64(4)	3.91(4)	-0.60(4)
O1	17.8(4)	22.9(4)	14.3(3)	1.6(3)	2.7(3)	-7.6(3)
O2	18.9(4)	20.6(4)	24.8(4)	2.7(3)	9.9(3)	0.1(3)
O3	23.6(5)	35.5(6)	36.8(6)	5.2(5)	-6.9(4)	-4.7(4)
N1	14.4(3)	13.9(3)	13.2(3)	-0.6(3)	3.2(3)	-1.4(3)
N2	16.7(4)	15.1(4)	16.4(4)	0.6(3)	4.4(3)	-0.5(3)
N3	16.2(4)	15.0(4)	18.0(4)	0.7(3)	3.2(3)	-0.8(3)

N4	16.2(4)	27.4(6)	45.9(7)	8.1(5)	7.5(5)	-0.7(4)
C1	13.9(4)	18.5(4)	14.5(4)	0.0(3)	3.6(3)	-2.6(3)
C2	13.7(4)	16.8(4)	14.6(4)	-1.0(3)	3.1(3)	-1.6(3)
C3	15.1(4)	18.0(4)	16.0(4)	-1.0(3)	4.3(3)	-2.4(3)
C4	15.6(4)	17.0(4)	16.3(4)	-0.2(3)	3.1(3)	-2.9(3)
C5	19.7(5)	18.2(5)	16.4(4)	-2.1(4)	3.6(4)	-3.1(4)
C6	17.4(4)	19.7(5)	14.4(4)	-1.6(3)	4.2(3)	-1.5(4)
C7	20.0(5)	17.6(5)	19.5(4)	0.2(4)	5.9(4)	-3.6(4)
C8	35.4(7)	26.9(6)	19.7(5)	3.0(5)	5.1(5)	-7.0(5)
C9	25.5(7)	25.2(7)	64.7(11)	4.5(7)	21.1(7)	-3.3(5)
C10	38.8(7)	25.8(6)	21.2(5)	-3.0(5)	7.8(5)	-15.0(6)
C11	26.6(6)	25.4(6)	20.9(5)	-5.0(4)	11.6(4)	-3.3(5)
C12	13.9(4)	16.7(4)	14.7(4)	-0.8(3)	3.7(3)	-1.1(3)
C13	19.0(5)	17.1(4)	14.1(4)	1.2(3)	5.6(3)	-1.3(4)
C14	17.4(4)	15.4(4)	15.7(4)	0.8(3)	3.6(3)	-1.9(3)
C15	25.4(5)	17.4(5)	21.3(5)	3.2(4)	7.0(4)	-2.5(4)
C16	28.6(6)	14.4(5)	27.4(6)	2.6(4)	7.0(5)	-0.3(4)
C17	25.9(6)	16.1(5)	27.2(6)	-0.1(4)	7.1(5)	2.2(4)
C18	20.0(5)	17.1(5)	21.5(5)	0.0(4)	6.5(4)	1.3(4)
C19	18.7(4)	16.4(4)	15.1(4)	-2.7(3)	4.6(3)	-1.1(4)
C20	15.3(4)	16.2(4)	17.5(4)	-1.8(3)	1.9(3)	-0.1(3)
C21	21.2(5)	16.3(5)	24.0(5)	-3.7(4)	2.7(4)	1.1(4)
C22	24.5(6)	13.8(5)	31.1(6)	-0.9(4)	1.4(5)	0.6(4)
C23	26.2(6)	16.0(5)	30.1(6)	3.9(4)	5.4(5)	-2.2(4)
C24	21.6(5)	16.7(4)	22.4(5)	3.2(4)	5.8(4)	-0.8(4)
C25	24.8(5)	22.0(5)	17.6(5)	4.6(4)	3.2(4)	-1.2(4)
S1	18.59(12)	19.89(12)	15.56(11)	0.51(9)	5.71(9)	2.38(10)
F1	31.5(5)	45.0(6)	45.8(6)	1.9(5)	0.9(4)	20.1(4)
F2	43.5(6)	57.9(7)	17.3(4)	-1.3(4)	0.9(4)	7.3(5)
F3	31.8(5)	40.2(6)	46.3(6)	-3.8(5)	6.3(4)	-13.2(4)
O4	33.8(5)	22.5(4)	17.3(4)	0.2(3)	10.4(3)	4.7(4)
O5	34.0(6)	30.1(5)	33.0(5)	3.4(4)	13.9(4)	-7.2(4)
O6	26.0(5)	30.9(5)	23.5(4)	-1.3(4)	7.1(4)	12.0(4)
C26	22.5(5)	29.5(6)	22.2(5)	-0.5(5)	3.3(4)	4.2(5)

References

1) Stoll, S.; Schweiger, A. *J. Magn. Reson.* **2006**, *178*, 42.
(2) Lionetti, D.; Day, M. W.; Agapie, T. *Chem. Sci.* **2013**, *4*, 785.
(3) Schopfer, M. P.; Mondal, B.; Lee, D.-H.; Sarjeant, A. A. N.; Karlin, K. D. *J. Am. Chem. Soc.* **2009**, *131*, 11304.
(4) APEX2, Version 2 User Manual, M86-E01078,; Bruker Analytical X-ray Systems: Madison, WI, June 2006.
(5) Sheldrick, G. M.; University of Göttingen: 2008.
(6) Sheldrick, G. M. Acta Crystallogr., Sect. A: Found. Crystallogr. **2008**, *64*, 112.